ELSEVIER

Ultramicroscopy 89 (2001) 177–188

ultramicroscopy

www.elsevier.com/locate/ultramic

Analysis conditions of an industrial Al–Mg–Si alloy by conventional and 3D atom probes ☆

F. Danoix[a,*], M.K. Miller[b], A. Bigot[c]

[a] *Groupe de Physique des Matériaux, UMR 6634, Faculté des Sciences, Université de Rouen, Place Emile Blondel, 76821, Mont Saint Aignan Cedex, France*

[b] *Microscopy and Microanalytical Sciences Group, Metals and Ceramics Division, Oak Ridge National Laboratory, P.O. Box 2008, Oak Ridge, TN 37831-6376, USA*

[c] *Pechiney CRV, Parc économique Centr'Alp, BP 27, 38 341 Voreppe CEDEX, France*

Received 18 July 2000; accepted 5 November 2000

Abstract

Industrial 6016 Al–Mg–Si(Cu) alloys are presently regarded as attractive candidates for heat treatable sheet materials. Their mechanical properties can be adjusted for a given application by age hardening of the alloys. The resulting microstructural evolution takes place at the nanometer scale, making the atom probe a well suited instrument to study it.

Accuracy of atom probe analysis of these aluminium alloys is a key point for the understanding of the fine scale microstructural evolution. It is known to be strongly dependent on the analysis conditions (such as specimen temperature and pulse fraction) which have been widely studied for 1D atom probes. The development of the 3D instruments, as well as the increase of the evaporation pulse repetition rate have led to different analysis conditions, in particular evaporation and detection rates. The influence of various experimental parameters on the accuracy of atom probe data, in particular with regard to hydride formation sensitivity, has been reinvestigated.

It is shown that hydrogen contamination is strongly dependent on the electric field at the specimen surface, and that high evaporation rates are beneficial. Conversely, detection rate must be limited to smaller than 0.02 atoms/pulse in order to prevent drastic pile-up effect. © 2001 Elsevier Science B.V. All rights reserved.

Keywords: Al–Mg–Si; 3D atom probe; Analysis conditions

1. Introduction

Aluminium 6xxx (Al–Mg–Si) family alloys are widely used as structural materials because of their high strength-to-weight ratio. Their mechanical properties can be finely adjusted by controlling the alloy composition and the precipitation sequence occurring at room and/or low temperature (i.e., $<200°C$). Small variations in the alloy composition lead to sensitive differences in the

☆ Research at the Oak Ridge National Laboratory SHaRE User Facility was sponsored by the Division of Materials Sciences and Engineering, US Department of Energy, under contract number DE-AC05-00OR22725 with UT-Battelle, LLC and through the SHaRE Program under contract DE-AC05-76OR00033 with Oak Ridge Associated Universities.

*Corresponding author. Tel.: +33-2-35-14-66-42; fax: +33-2-35-14-66-52.

E-mail address: frederic.danoix@univ.rouen.fr (F. Danoix).

0304-3991/01/$ - see front matter © 2001 Elsevier Science B.V. All rights reserved.
PII: S0304-3991(01)00098-5

precipitation sequence, and therefore in the mechanical properties. As the resulting finely dispersed precipitates are on the nanometer scale, the atom probe is a unique instrument to study their size, number density and compositional evolution with ageing treatment. In order to correlate microstructural and mechanical data, it is important to determine quantitatively the chemical composition with the atom probe.

Aluminium based alloys pose special problems during atom probe analysis due to their low evaporation field combined with aluminium's monoisotopic nature. The low evaporation field favours the formation of aluminium hydrides (and possibly hydrides of other alloying elements). It is therefore necessary to ensure that the probability of hydride formation is as low as possible by controlling the experimental parameters such as specimen temperature or pulse fraction.

1.1. Hydrides formation

In the case of singly charged aluminium hydrides $(AlH_x)^+$, additional peaks appear in the mass spectrum at 28, 29 and sometimes at 30 u.m.a. In the case of energy-compensated instruments, their presence will affect the estimate and even possibly the detection of iron, as the main mass-to-charge peaks of iron are at 27 and 28 amu. In the case of non-energy-compensated instruments, detection of Fe^{2+}, Mn^{2+}, and possibly Cu^{2+}, added as minor alloying element, is problematic. As these elements form dispersoids, they are not supposed to be present in the matrix, whereupon they influence the decomposition sequence. Thus, their quantification by atom probe will not be considered in this work. More problematic is the case of the doubly charged aluminium hydrides $(AlH_x)^{2+}$, as the additional peaks would superimpose on the $^{28}Si^{2+}$ peaks at 14, 14.5 and 15 amu. This effect can be of particular importance as a 1% $(AlH)^{2+}$ addition to the $^{28}Si^{2+}$ peak would not only result in a doubling of the measured silicon content but also lead to a misinterpretation of this solute distribution in the material. This possible overlap between $^{28}Si^{2+}$ and $(AlH)^{2+}$ has been ruled out in the case of low (<0.1at%) Si content Al–Zn–Mg alloy [1], and no evidence found in 6xxx alloys [2], hence no quantitative analysis has been published to date for this alloy family. The quantitative analysis of Si^{2+} isotopic ratio, which is the only way to estimate the importance of this overlap, will be examined, and the overlap importance estimated.

1.2. Aluminium loss

The second effect that may lead to systematic errors is the loss of aluminium. First possible cause is the ion pile-up effect. When two (or more) ions of the same mass-to-charge ratio strike the detector at the same time, there is a probability that one (or more) is not accounted for. This probability is strongly dependent on the nature of the detection system and on the mass resolution of the instrument. In that respect, the worst case would be a high mass resolution energy-compensated 1D atom probe (i.e. with a non-segmented detector) operated at a high detection rate. As ion pile-up is directly proportional to the relative abundance of the mass-to-charge peaks, the various peaks will be differently affected; the main peak being more affected than minor ones, leading to a bias in the measured composition. This effect is revealed, and may be partly corrected, for elements with multiple isotopes by comparing the measured and natural isotopic ratios. Since aluminium is by far the main constituent of 6xxx alloys, its concentration may be severely affected. Unfortunately, aluminium is monoisotopic, thus ion pile-up cannot be directly detected and corrected. Another potential source of aluminium loss is the preferential evaporation of aluminium, as it is a low evaporation field element. Again, this effect cannot be directly evidenced. In addition, preferential evaporation aluminium is rarely considered.

The consequence of aluminium loss is the simultaneous increase of the concentrations of all solute elements in the same proportion. Thus, the only way to ensure reliability of atom probe data is a direct comparison with the alloy nominal composition.

1.3. Experimental conditions

The accuracy of atom probe analysis of 6xxx aluminium based alloys is known to be severely

sensitive to analysis conditions. A review of the literature shows a general consensus that the experimental conditions required are a specimen temperature of lower than 40 K and a pulse to a standing voltage ratio of ~20% [3,4]. These conditions were determined when 1D atom probes were used. Different types of atom probes (1D and 3D, conventional and energy compensated) are now being used, with different detection systems (single or multi-hit capabilities) and evaporation conditions (small or large acceptance angles), potentially leading to differences in the instrument performance. In this study, the influence of the various experimental parameters in terms of quantitative analysis, will be examined for a 6016 aluminium alloy.

2. Experimental

The alloy used in this study is a commercial 6016 alloy, provided by Pechiney, and referenced as HF100 [5]. Its composition is given in Table 1. Otherwise stated, studied samples are in the as received condition, i.e. they only experienced room temperature ageing, for periods up to 18 months. In this state, only GP zones with a higher number of density ($>10^{19}\,cm^{-3}$) are observed. Provided that the analysed volume is sufficiently large ($>10^3\,nm^3$, or >5000 ions), local concentration fluctuations are averaged and no compositional fluctuations are expected.

Three different instruments have been used, the tomographic atom probe (TAP [6]), the ORNL energy-compensated optical position-sensitive atom probe (ECOPoSAP [7]) and the Rouen 1D energy-compensated atom probe [8]. All three instruments allow specimen temperature as low as 20–25 K and have hydrogen partial pressure in the range 10^{-11}–10^{-12} mbar. The TAP and ECOPoSAP have similar acceptance angles (respectively, 88 and 72 mrad). For both instruments, the analysed surface is proportional to the square of the applied voltage, thus it increases during analysis. The evaporation and detection rates do not follow the same evolution, resulting in non-stationary analysis conditions. This effect may be particularly important when the specimen voltage varies significantly, e.g., if the voltage increases by a factor of 3, the evaporation over detection rate ratio changes by one order of magnitude. Conversely, the 1D atom probe is equipped with a variable iris [9], that allows both rates to be kept proportional, or to be modified independently. It should be noted that a stationary evaporation rate could be achieved under software control in the TAP and ECOPoSAP; however, this was not done in this study. 3D instruments were preferred when isotopic ratios were examined, because a significantly larger number of ions were collected. On the other hand, the 1D instrument was used to study the influence of experimental conditions, in particular of the detection and evaporation rates.

Mass spectra for all three instruments are shown in Fig. 1. It is evident that the mass resolution of the TAP is too low to allow singly charged aluminium hydrides to be clearly resolved from the aluminium, and to a lesser extent doubly charged aluminium and silicon. Thus, the TAP has not been used to study the influence of experimental conditions, but the conclusions drawn from the ECOPoSAP under the same experimental conditions can apply to it.

In standard conditions, all instruments are used in a remote control mode, with a pulse repetition rate of 1500–1700 Hz, TAP and ECOPoSAP with detection rates in the range 0.01–0.1 atom/pulse, in the range 0.001–0.02 for 1DAP.

Table 1
Alloy composition, as given by Pechiney [5], and as measured with the different instruments used

Element	Al	Mg	Si	Cu	Fe	Mn
Bulk (at%)	98.30	0.33	1.16	0.06	0.10	0.05
Solid solution (at%) (dispersoids and eutectic particles free)	98.74	0.33	0.87	0.06	—	—
Solid solution (at%) ECOPoSAP	98.14	0.48	1.22	0.16	—	—
Solid solution (at%) 1D ECAP	98.56	0.31	1.07	0.04	—	—

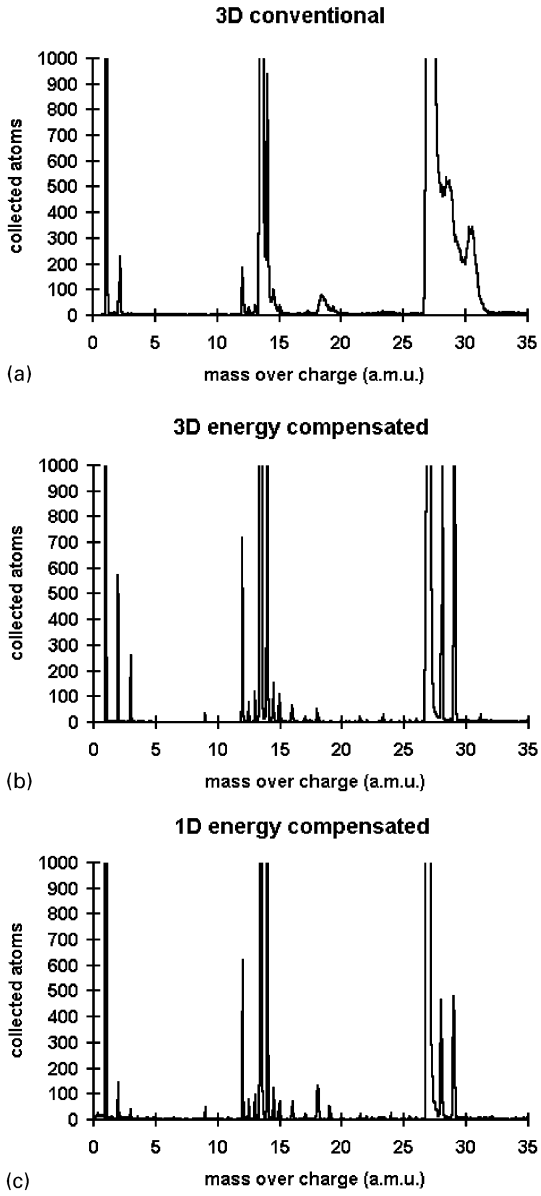

Fig. 1. Mass spectra of the instruments used, (a) TAP, (b) ECOPoSAP and (c) 1DAP.

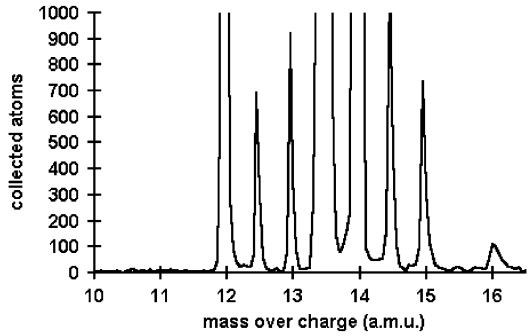

Fig. 2. Enlarged mass spectrum obtained in the EcoPoSAP.

3. Results and discussion

3.1. Magnesium and silicon isotopic ratios

The mass peaks for Mg, Si, and Al^{2+} are located in the 12–15 amu mass-to-charge range and are separated by 0.5 amu, as shown in Fig. 2. In order to study the Mg and Si isotopic ratios, it is therefore important to separate each peak unambiguously. The measured and natural isotopic ratios for magnesium and silicon are given in Table 2. The measured data were obtained by cumulating all data sets from ECOPoSAP and 1 DAP runs. Two main discrepancies appear in this table. The third (and last) isotopes of both Mg and Si are overestimated. As the abundances of the second isotopes are identical to the natural ones, within the 2σ confidence level, the presence of parasite ions at 13 and 15 amu is indicated (Table 3).

Detailed examination of the different data sets reveals three types of analysed domains: copper layers at the beginning of the runs, followed by solid solution analysis, and sometimes by solid solution domains after a small flash occurred (Table 3).

3.1.1. Copper layers

Most of the analyses were started without prior FIM imaging. As a result, an initial copper enriched surface layer was systematically detected as shown in Fig. 3a. The origin of this surface layer is probably due to copper deposition after electropolishing, the presence of copper in the electrolyte resulting from anodic dissolution of the specimen. The distribution of oxygen in this copper layer was investigated, as shown in Fig. 3b. The amount of oxygen is 0.05 at%, ruling out the presence of any copper oxide layer. After the copper layer was evaporated, solid solution could be successfully analysed with a high success rate (> 75%). As no detrimental alumina layer was observed, it is likely

Table 2
Isotopic ratios for Mg and Si for 3D and 1D energy compensated instruments

Isotope		$^{24}Mg^{2+}$	$^{25}Mg^{2+}$	$^{26}Mg^{2+}$	$^{28}Si^{2+}$	$^{29}Si^{2+}$	$^{30}Si^{2+}$
Natural isotopic ratio (%)		78.99	10.00	11.01	92.23	4.67	3.10
3D	Detected ions	10,940	1398	2282	45,731	2254	2004
	Measured isotopic ratio (%)	74.91	9.46	15.63	90.94	5.08	3.98
	2σ (%)	0.72	0.48	0.60	0.26	0.20	0.17
1D	Detected ions	1692	239	290	6907	386	299
	Measured isotopic ratio (%)	76.18	10.76	13.06	90.98	5.08	3.84
	2σ (%)	0.86	0.64	0.66	0.31	0.24	0.20

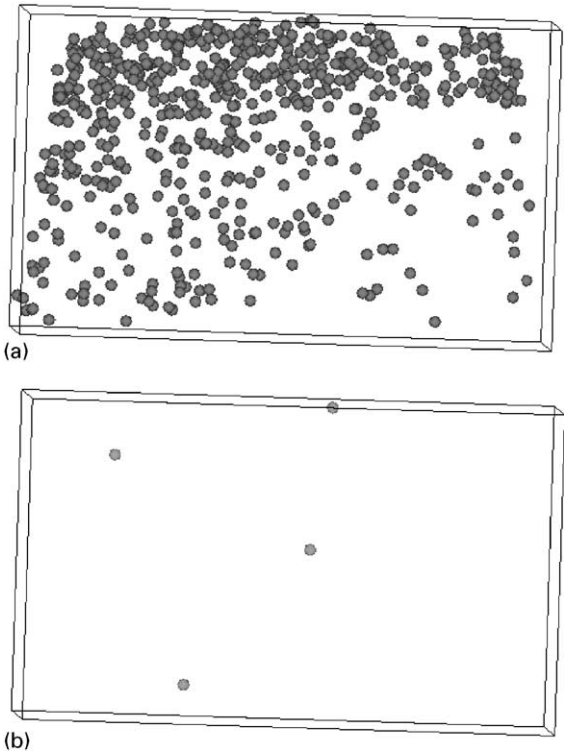

Fig. 3. A 3D reconstruction of a copper enriched top layer ($17 \times 17 \times 11\,nm^3$): (a) copper and (b) oxygen.

that this copper layer partly protects the specimen from oxidation. Thus, these copper layers could be deliberately formed for protective purposes.

The surface layer consists of a few nanometer thick high copper content (up to 75 at% Cu) region, followed by a copper content decrease to the bulk level. The volumes selected as 'copper layers' were delimited to incorporate all copper-enriched regions, i.e. the layer itself and the gradient region. As a consequence, the corresponding composition, given in Table 3, is convoluted with the matrix one. Solute element concentrations are much higher than expected, in particular for Si and Cu. As shown in Fig. 4, copper is mainly detected as $(CuH_2)^{2+}$. This mass spectrum also shows the presence of Al^{3+}, usually indicating the presence of oxide [10], even though no oxide layer was found. Isotopic ratios are given in Table 4. A strong enhancement of $^{26}Mg^{2+}$ is observed, which is probably due to $^{24}MgH_2^{2+}$. Conversely, it is observed that the main Si isotope is favoured, which in turn may indicate the presence of AlH^{2+}.

3.1.2. After flash volumes

A large majority of specimen ended by a flash. Minor flashes may not destroy the specimen. The main evidence of a minor flash is a rapid voltage increase. As shown in Fig. 5, mass spectra obtained after flashes are very similar to those of the solid solution analysis (see Fig. 6). The only significant effect on measured composition, as given in Table 3, is an enhancement of the copper content. Copper is mainly detected as CuH_2^+. Concerning Mg and Si isotopic ratios (Table 5), only the third isotopes are favoured, giving evidence for the same Mg and Si di-hydrides as in the copper layer. As specimen flashes may not be noticed during remotely controlled analyses, but affect composition measurements, voltage evolution should be checked before data processing.

Table 3
Compositions obtained with the ECOPoSAP

Element	Al	Mg	Si	Cu
Bulk	98.74	0.33	0.87	0.06
Average	98.09±0.01	0.40±0.01	1.25±0.01	0.26±0.01
Copper layers	93.73±0.08	0.64±0.03	2.96±0.05	2.67±0.05
Flashed volumes	98.17±0.01	0.17±0.01	1.22±0.01	0.45±0.01
Clean volumes	98.14±0.01	0.48±0.01	1.22±0.01	0.16±0.01

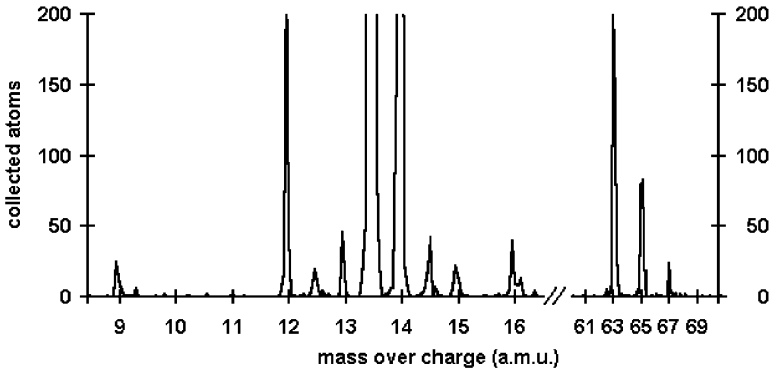

Fig. 4. Cumulative mass spectrum of the surface copper layers.

Table 4
Isotopic ratios in the copper layers (calculated over 70,000 ions)

Isotope	$^{24}Mg^{2+}$	$^{25}Mg^{2+}$	$^{26}Mg^{2+}$	$^{28}Si^{2+}$	$^{29}Si^{2+}$	$^{30}Si^{2+}$
Measured isotopic ratio (%)	74.53	9.91	15.57	93.71	3.93	2.35
Standard deviation (σ) (%)	2.12	1.45	1.76	0.55	0.44	0.34
Natural isotopic ratio (%)	78.99	10.00	11.01	92.23	4.67	3.10

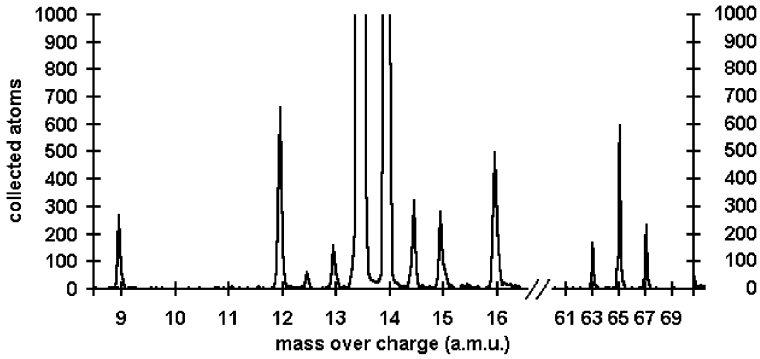

Fig. 5. Cumulative mass spectrum of analyses performed after flashes.

Table 5
Isotopic ratios in the after flash volumes (900,000 ions)

Isotope	$^{24}Mg^{2+}$	$^{25}Mg^{2+}$	$^{26}Mg^{2+}$	$^{28}Si^{2+}$	$^{29}Si^{2+}$	$^{30}Si^{2+}$
Measured isotopic ratio (%)	65.80	8.02	26.18	89.75	5.22	5.02
Standard deviation (σ) (%)	1.25	0.72	1.17	0.30	0.22	0.21
Natural isotopic ratio (%)	78.99	10.00	11.01	92.23	4.67	3.10

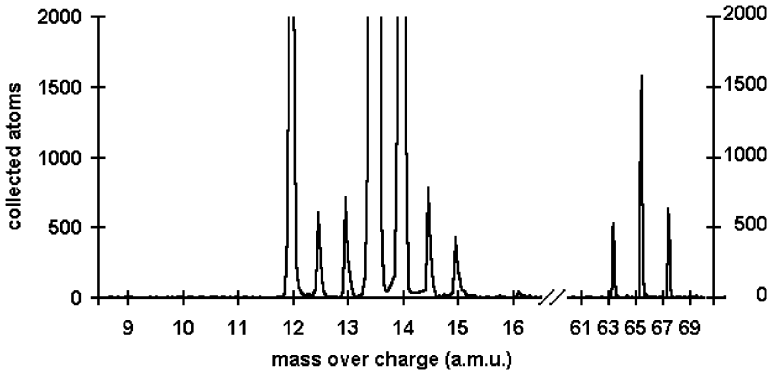

Fig. 6. Cumulative mass spectrum of solid solution analyses.

3.1.3. Solid solution

With all the copper layers and post-flash volumes being taken away, only solid solution analysis remained. The corresponding mass spectrum (Fig. 6) shows that copper is detected mainly as copper di-hydrides. The Mg isotopic ratio again shows an enhancement of the third isotope ratio, giving evidence that a proportion of $(MgH_2)^{2+}$ formation during analysis. Its amount can be estimated (from the peak at 13 amu height) to be approximately 3% of the $^{24}Mg^{2+}$ peak. As this ratio must be constant for all isotopes, 0.5% of the total Mg content may be lost, due to $^{25}(MgH_2)^{2+}$ and $^{26}(MgH_2)^{2+}$ peak shifts to Al^{2+} and $^{28}Si^{2+}$ mass peaks. As Mg concentration is about 0.3%, the uncertainty on Mg content will only be 0.0015 at%, much smaller than the uncertainty due to the detection efficiency, and thus not considered. The Si isotopic ratios (Table 6) are in excellent agreement with the natural abundances, indicating that no Al hydrides are detected in the $^{28}Si^{2+}$ peak. This result is important, as it indicates that silicon content can be estimated accurately by atom probe. The solute element concentration also appears higher than that expected from bulk composition analysis. As the measured Mg/Si ratio (0.39) is closer to the expected one (0.38), aluminium loss, either by preferential evaporation, or more likely by ion pile-up, must be responsible for this enhancement. The experimental conditions used with this 3D atom probe lead to an overestimation of both Mg and Si contents, probably because of aluminium ion pile-up effect. Thus, a detailed study of the influence of the experimental conditions on the accuracy of the atom probe data was undertaken with a 1D instrument.

3.2. Analysis conditions

The influence of analysis conditions on the measured compositions has been studied for the same 6016 alloys. In order to control all experimental parameters, the Rouen energy-compensated 1D atom probe was used. Its main advantage is to allow the remote control of the analysed surface (as seen from the detector), which is kept constant by reducing the entrance window of the

Table 6
Isotopic ratios in the solid solution (3×10^6 ions)

Isotope	$^{24}Mg^{2+}$	$^{25}Mg^{2+}$	$^{26}Mg^{2+}$	$^{28}Si^{2+}$	$^{29}Si^{2+}$	$^{30}Si^{2+}$
Measured isotopic ratio (%)	**77.12**	9.96	12.92	91.56	5.18	3.26
Standard deviation (σ) (%)	0.41	0.29	0.32	0.17	0.15	0.12
Natural isotopic ratio (%)	78.99	10.00	11.01	92.23	4.67	3.10

Poschenreider lens as the specimen voltage was increased. Thus, detection and evaporation (defined as the number of evaporated ions per specimen unit surface and per pulse, and directly proportional to the analysed surface) rates can be kept constant simultaneously.

Another important advantage of this instrument is that it allows the variation of the evaporation rate, independent of the detection rate, and vice versa. Despite the major influence of these two experimental parameters on the analysis conditions (respectively, ion pile-up and hydrogen contamination), they have not been studied independently. The main reason is that, on most instruments, these two parameters are normally not varied independently. For most instruments, in particular all 3D ones, the analysed surface increases during analysis, as the square of the applied voltage, leading to a different evolution of the detection and evaporation rates. With the 1D instrument, when only the detection rate is to be changed, the remote control instruction is modified, and the iris is adjusted in order to maintain the analysed surface, thus the evaporation rate, remains constant. For example, if the detection rate is increased by a factor of 4, then the iris is enlarged by a factor of 2. The iris may be opened in order to reduce the evaporation rate or closed to increase it.

For each run reference analyses were conducted with a specimen temperature of 40 K, 19% pulse fraction, pulse repetition rate of 1700 Hz (constant, whatever the detection rate was), and with a diameter of the analysed surface of 4 nm. Then, only the experimental parameter under investigation was modified, and the results were compared with those of the corresponding reference analysis.

Composition (Table 1) and isotopic ratios (Table 3) measured with the 1D atom probe in the reference conditions are closer to the expected ones than those obtained with the 3D atom probe, as a consequence of different analysis conditions.

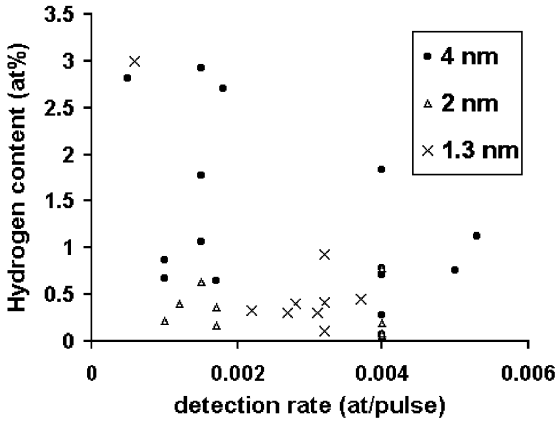

Fig. 7. Hydrogen content in 1DAP analyses as a function of the detection rate. The different symbols represent different diameters of the surface analysis used.

3.2.1. Hydrogen content

All reference analyses conducted with various detection rates have been gathered. As shown in Fig. 7, a large scatter in the hydrogen content from one run to another is observed. The reason for different hydrogen contaminations of the specimen is not clear. As all runs were conducted on the same instrument under the base vacuum conditions, it is unlikely to be a residual vacuum effect. The shape of the specimens, mainly the shank angle, could also be responsible for hydrogen contamination as it strongly influences the field at the specimen apex. TEM examinations of specimen shank angle prior to AP analysis have been performed by Warren, and no obvious correlation between hydrogen contamination and shank angle was observed [11]. Another possible source of hydrogen contamination is electropolishing, but

no experimental evidence has been found. As hydrogen content is a key point of this work, the direct comparison between data obtained from different specimens is not possible. Thus when experimental conditions were modified, only data obtained on individual specimens were used for comparison, and are indicated by double lines in the following tables. As a consequence, the influence of different experimental conditions have been studied on different specimens, and a direct comparison of absolute concentration and hydrogen content is not relevant.

3.2.2. Temperature

Results obtained for different specimen temperatures are given in Table 7. Two different specimens have been analysed, leading to large differences in the hydrogen contamination levels. From the first specimen, it appears that the increase of the specimen temperature provokes an important increase of the hydrogen contamination. This effect is not observed on the second specimen, where contamination is negligible for all temperatures. Reducing the temperature from 40 to 20 K does not affect the measurements of the solute elements. However, the solute contents are high compared to the bulk composition. As no evolution is observed with temperature, and other analysis conditions being standard, it is believed that these values are representative of this specimen concentration. Conversely, increasing the temperature from 40 to 80 K significantly increases the solute content, in particular for Si. As the detection rate was kept constant, solute overestimation cannot be attributed to aluminium loss by ion pile-up. It can thus be attributed to preferential evaporation of aluminium, indicating a lowering of the mean field at the surface, as expected when the specimen temperature is increased. This is consistent with the observed increase in hydrogen contamination. As the field is lowered, hydrogen is more likely to reach the specimen apex before being ionised and/or repelled.

Therefore, it appears that 40 K is the highest temperature that should be used for quantitative analysis of this 6016 aluminium alloy.

3.2.3. Pulse fraction

Results obtained for different pulse fractions are given in Table 8. The pulse fraction clearly influences both the quantitativity and the hydrogen

Table 7
Influence of the specimen temperature

Temperature (K)	Detection rate (at/pulse)	Mg (at%)	Si (at%)	$(AlH_x)^+$ (at%)	$(H_x)^+$ (at%)	Mg/Si
80	0.0015	0.55±0.20	1.89±0.20	7.94±0.39	2.92±0.24	0.29
60	0.0015	0.59±0.08	1.21±0.11	3.90±0.19	1.78±0.13	0.49
40	0.0015	0.34±0.04	0.85±0.06	1.31±0.08	1.06±0.07	0.4
40	0.0012	0.48±0.05	1.27±0.10	0.09±0.03	0.19±0.03	0.38
32	0.0012	0.45±0.06	1.29±0.10	0.09±0.03	0.21±0.04	0.35
24	0.0012	0.50±0.07	1.20±0.11	0.07±0.03	0.24±0.05	0.41
20	0.0012	0.48±0.07	1.24±0.11	0.08±0.03	0.18±0.04	0.39

Table 8
Influence of the pulse fraction

Pulse fraction (V_{pulse}/V_{DC}) (%)	Detection rate (at/pulse)	Mg (at%)	Si (at%)	$(AlH_x)^+$ (at%)	$(H_x)^+$ (at%)	Mg/Si
19	0.0032	0.26±0.03	0.69±0.05	0.72±0.13	0.93±0.11	0.38
12	0.0032	0.11±0.03	0.68±0.08	0.12±0.03	0.10±0.03	0.16
19	0.0017	0.35±0.05	0.99±0.08	0.42±0.06	0.37±0.05	0.36
12	0.0017	0.23±0.04	1.11±0.09	0.10±0.03	0.17±0.03	0.21

contamination. For a 19% pulse fraction, Mg and Si contents are rather similar to the expected ones, as well as the Mg/Si ratio. The main effect of pulse fraction lowering is a magnesium content underestimation, and a decrease of hydrogen contamination. This last effect can be explained, as lowering pulse fraction increases the standing field at the specimen surface, and thus reduces hydrogen contamination. The effect on solute content is not understood. As only Mg (and therefore Mg/Si ratio) is affected, it cannot be due to a simple difference in aluminium evaporation. In addition, if preferential evaporation of Mg would take place, then it should also be observed for Al. The stability of measured silicon content rules out this possibility.

3.2.4. Pulse repetition rate

Results obtained for different pulse repetition rates are given in Table 9. The main consequence of reducing the pulse repetition rate is an increase of the hydrogen contamination. Reducing the pulse repetition rate from 1700 to 88 Hz does not significantly affect the mean value of the field value at the specimen surface, but reduces by a factor of 20 the period time between two pulses when the specimen experiences the lower field. It is thus concluded that the important aspect regarding hydrogen contamination is the time left for hydrogen to migrate to the specimen apex, and/or combine with the surface atoms. The measured solute contents are not affected by the pulse repetition rate.

3.2.5. Detection rate

Results obtained for different detection rates are given in Table 10. For this experiment, the reference analysis was first performed with a low evaporation rate to prevent any significant pile-up. The analysis was then conducted with a detection rate 16 times higher, and an analysed area 16 times larger. The evaporation conditions were thus kept constant. The stability of hydrogen contamination confirms that it is directly dependent on the evaporation conditions. Increasing the detection rate increases the solute content. This effect can be interpreted in terms of Al loss by pile-up that artificially raises the measured solute concentrations. The selected detection rate was chosen to be similar to the one used with the 3D instruments, and similar solute contents are detected. Even if multi-hit capabilities of the various instruments are different, leading to different sensitivities to ion pile-up, a detection rate of 0.02 ion per pulse appears to be too high for energy-compensated instruments.

3.2.6. Evaporation rate

Results obtained for different evaporation rates are given in Table 11. The evaporation rate was

Table 9
Influence of the pulse repetition rate

Pulse repetition rate (Hz)	Detection rate (at/pulse)	Mg (at%)	Si (at%)	$(AlH_x)^+$ (at%)	$(H_x)^+$ (at%)	Mg/Si
1700	0.005	0.39±0.12	1.45±0.20	0.41±0.11	0.41±0.09	0.27
88	0.005	0.38±0.08	1.08±0.12	4.52±0.41	3.25±0.24	0.35
1700	0.005	0.39±0.06	1.63±0.11	0.03±0.01	0.12±0.03	0.24
1100	0.005	0.35±0.05	1.53±0.10	0.09±0.02	0.16±0.03	0.23
430	0.005	0.41±0.09	1.64±0.18	0.20±0.09	0.39±0.09	0.25

Table 10
Influence of the detection rate

Detection rate (at/pulse)	Mg (at%)	Si (at%)	$(AlH_x)^+$ (at%)	$(H_x)^+$ (at%)	Mg/Si
0.0012	0.28±0.02	1.04±0.04	0.18±0.02	0.40±0.02	0.27
0.02	0.46±0.05	1.41±0.09	0.16±0.03	0.49±0.02	0.32

Table 11
Influence of the evaporation rate

Diameter of the analysed surface (nm)	Detection rate (at/pulse)	Mg (at%)	Si (at%)	$(AlH_x)^+$ (at%)	$(H_x)^+$ (at%)	Mg/Si
8	0.001	0.36±0.07	1.33±0.14	0.98±0.11	1.26±0.13	0.27
4	0.001	0.31±0.10	1.25±0.19	1.04±0.16	0.67±0.14	0.25
2	0.001	0.27±0.04	1.20±0.09	0.45±0.06	0.22±0.04	0.23
8	0.005	0.55±0.07	1.27±0.10	0.16±0.03	0.08±0.03	0.43
4	0.005	0.35±0.08	1.01±0.15	0.07±0.04	0.07±0.02	0.35
2	0.005	0.34±0.06	1.04±0.10	0.08±0.03	0.05±0.02	0.33

increased by reducing the analysed surface and maintaining the detection rate constant. As the diameter of the analysed surface is reduced by a factor of 2, the evaporation rate is multiplied by a factor of 4. These results, obtained on two different specimens, again give evidence that hydrogen contamination is highly dependent on the evaporation rate. This is clearly demonstrated with the first specimen, which was more affected by contamination. These results are confirmed with the second specimen, even though the trend is less significant. There is no obvious effect on solute concentration even though a small increase is observed with the lower evaporation rate. Preferential evaporation of aluminium could be suspected, but more data are necessary for confirmation.

4. Conclusion

Factors affecting quantitative atom probe analysis of a 6016 Al–Mg–Si alloy have been studied in detail. These results show that hydrogen contamination is strongly dependent on the electric field conditions at the specimen surface. When the field is increased by raising the evaporation rate, then hydrogen content is reduced. Experimental data indicate that contamination takes place when the specimen experiences the standing field, i.e. when no evaporation pulse is applied. Indeed, when the difference between standing and pulse fields is lowered (either by reducing the specimen temperature or the pulse fraction), so is hydrogen contamination. In addition, a kinetic aspect is evidenced, as contamination is reduced when the pulse repetition rate is increased. The important parameter is the time that the specimen spends at standing field between the evaporation pulses during which the hydrogen may migrate and/or combine with surface atoms. When this period is shorter, then contamination is greatly reduced.

Concerning ion pile-up, it has been shown quantitatively that a detection rate of 0.02 atoms/pulse is too high, and affects composition measurements. As multi-hit capabilities are different from one instrument to the other, a detailed analysis of ion pile-up should be conducted independently on each instrument.

It has been shown that high evaporation rates are beneficial for atom probe analysis of aluminium alloys, but are limited by the multi-hit capabilities of present detectors. A future development of detection systems should take into account the need for significantly higher detection rates.

References

[1] K. Stiller, P.J. Warren, V. Hansen, J. Angenete, J. Gjonnes, Mater. Sci. Eng. A 270 (1999) 55–63.
[2] A. Bigot, Ph.D. Thesis, University of Rouen, March 1998.
[3] G.A. Edwards, K. Srtiller, G.L. Dunlop, Appl. Surf. Sci. 76/77 (1994) 219–225.
[4] M. Murayama, K. Hono, Acta Mater. 47 (1999) 1537–1548.
[5] R. Shahani, D. Daniel, J.C. Ehrström, J.L. Hoffhann, B. Grange, in: D. Das (Ed.), Proceedings of "automotive Alloys 1999" – TMS Annual Meeting, pp. 193–204.
[6] D. Blavette, B. Deconihout, A. Bostel, J.M. Sarrau, M. Bouet, A. Menand, Rev. Sci. Instrum. 64 (1993) 2911–2919.

[7] A. Cerezo, T.J. Godfrey, S.J. Sijbrandij, G.D.W. Smith, P.J. Warren, Rev. Sci. Instrum 69 (1998) 49–58.
[8] J.M. Sarrau, F. Danoix, M. Bouet, B. Deconihout, D. Blavette, A. Menand, Appl. Surf. Sci. 76/77 (1994) 367–373.
[9] F. Danoix, M. Bouet, P. Pareige, A. Menand, Appl. Surf. Sci. 67 (1993) 451–458.
[10] K. Stiller, private communication.
[11] P.J. Warren, private communication.